

Nanocomposites Based on Aromatic Polyesters and Organically Modified Clay

G. Engelmann, E. Bonatz, J. Ganster

Fraunhofer – Institute for Applied Polymer Research, Geiselbergstraße 69, Potsdam-Golm 14476, Germany

Correspondence to: G. Engelmann (E-mail: gunnar.engelmann@iap.fraunhofer.de)

ABSTRACT: Milled polybutylene terephthalate (PBT) and polytrimethylene terephthalate (PTT) were mixed with organically modified clay and extruded to prepare nanocomposites by melt intercalation. The modifier of the nanofiller belongs to the group of trialkylbenzylammonium cations. Manufacturing of the materials was carried out with a co-rotating twin-screw-extruder at 230°C and 240°C for PTT and PBT, respectively. A concentration of 3% of the inorganic filler component in the composites was aimed at. The influence of mechanical stress during extrusion on the stability of the neat polymers was tested at different speeds of rotation between 100 rpm and 800 rpm. The composites were characterized with regard to the experimental filler content and the properties of the matrix polymers like melt and crystallization temperatures, degrees of crystallinity, intrinsic viscosities, and melt viscosities. Additionally, mechanical properties were analyzed by tensile tests and discussed in terms of processing and the filler presence. The dominance of PBT as polymer matrix was highlighted. © 2012 Wiley Periodicals, Inc. *J. Appl. Polym. Sci.* 000: 000–000, 2012

KEYWORDS: polyesters; clay; nanocomposites; polymer extrusion

Received 14 April 2011; accepted 11 March 2012; published online 00 Month 2012

DOI: [10.1002/app.37680](https://doi.org/10.1002/app.37680)

INTRODUCTION

The development of nanocomposites can be separated into three main topics, which mutually depend on each other: the processing procedure, the fillers, and the interactions between filler and the composite matrix. Three techniques are mainly used to disperse nanofillers in the polymers, i.e., preparation from solution,^{1,2} *in situ* intercalation,^{3,4} and melt intercalation.⁵ From a practical point of view, melt intercalation is the more interesting alternative owing to the lack of solvents and the possibility of a continuous process.

The variable chemical structures of the nanofillers and their different geometrical dimensions impact mainly the properties of the corresponding nanocomposites. In contrast to spherical particles, nanofillers with large aspect ratios like double-layered hydroxides or layered silicates offer the chance for better barrier properties.⁶ Comparatively low concentrations of carbon nanotubes can increase the electrical conductivity of a composite after the formation of a percolating network.⁷ Although carbon nanotubes offer a wide variety of interesting perspectives, modified layer-structured fillers are commercially dominating. Most of them belong to the group of naturally occurring clays. Chemically modified clays can be prepared by exchanging the small inorganic cations against organic cations of comparably

high molecular weights.⁸ The galleries between the clay layers becomes expanded with a benefit for exfoliation.⁹ Additionally, the contact between the composite matrix and the platelets of the clays can be tailored by the polarity of these organic cations.¹⁰ This offers the chance to prevent agglomeration. The organic cations belong mainly to the groups of phosphonium,¹¹ imidazolium,¹² and especially alkylated ammonium¹³ cations. These cationic structures exert influence on thermal stability of both the modifiers and the modified clays.¹⁴

The repertoire of matrix polymers used for composite preparation is substantial.^{15,16} On the one hand side bio-based polymers or polymers made on bio-based monomers like PHB¹⁷ and starch¹⁸ or PLA,¹⁹ respectively, are of great interest. On the other hand, synthetic polymers like, polypropylene,²⁰ polyethylene,²¹ polyurethane,²² polycarbonate,²³ polystyrene,²⁴ polyamide 6,²⁵ and further polyamides²⁶ are in the focus of research activities. Aromatic polyesters like PTT, PBT, and PET^{27–29} can be classified as a special subgroup in this field. Up to now, polyethylene terephthalate (PET) and polybutylene terephthalate (PBT) dominate the polyester market. Main fields of application for PET are bottles, films,³⁰ and fibers³¹ and, with respect to PBT, divers equipment for electrical and automotive industries³² is produced. In contrast to PET and PBT, the production of polytrimethylene terephthalate (PTT) was not of economical

© 2012 Wiley Periodicals, Inc.

relevance. The too high price of 1,3-propanediol (PDO), contrary to 1,2-ethanediol or 1,4-butanediol, can be identified as the main reason. A new synthesis procedure for 1,3-propanediol means a breakthrough for the PTT-production. Shell-company manufacture PTT, named as Corterra,³³ based on chemically produced PDO. DuPont preferred the synthesis of 1,3-propanediol (bio-PDO) by fermentation of corn sugar. PTT derived from bio-PDO is labeled as Sorona.³⁴ PTT is mainly applied for the manufacturing of fibers and fiber-based products due to excellent colorability and softness.³⁵

Nevertheless, there is great interest to establish PTT as an engineering plastic, too. The necessary improvements of PTT properties for entering new markets are possible by compounding, for instance. Regardless of the wide variety of filler-types, nanofillers are of great interest for research activities. A general problem for PTT-based nanocomposites, studied in detail, is the influence of successfully dispersed nanofillers on crystallization behavior. Spherically structured CaCO₃-particles could be clearly highlighted as nucleating agents³⁶ as well as clay-based fillers modified by organic ammonium cations.^{37,38} Additionally, the influence of clay content on clay dispersion, polymer melting and crystallization was tested and an ideal concentration of 3% could be established.³⁷ Liu et al.³⁹ as well as Drown et al.⁴⁰ published on the influence of such important issues as chemical structure of the modifiers, ion-exchange capacity (IEC), and filler concentration on tensile and bending properties. In this case, an optimal range of the filler concentration between 2% and 3% was identified for an extended set of modified fillers. With regard to the preparation of PTT-based nanocomposites by melt-intercalation, various extrusion conditions were reported. In addition to the screw-design, processing temperatures (230–260°C) and screw rotational speeds (140–400 rpm) were varied. Generally, the sensitivity of neat and loaded aromatic polyesters compared to thermoplastic processing conditions is well known⁴¹ and a reduction in mechanical properties due to partial polymer degradation can not be excluded.

Focus of this article is to study the influence of selected extrusion conditions and an organically modified clay on the properties of the corresponding PTT-based nanocomposites, prepared by melt intercalation. As reference materials, the corresponding PBT-based nanocomposites were manufactured as well, with a PBT which was especially adapted to typical processing conditions of extrusion.

EXPERIMENTAL PART

Materials

PBT (Ultradur[®] B 6550) and PTT were used as purchased from BASF and PTT Poly Canada, respectively. The intrinsic viscosities of PBT and PTT are $\eta_0 = 1.277$ dL/g and $\eta_0 = 0.977$ dL/g (o-dichlorobenzene/phenol = 2 : 3), respectively. The used filler Nanofil 2 (bentonite, modified with benzyldimethylstearylammonium cations) was used as ordered from SüdChemie Co. Germany (average particle size: 11.3 μm).

Sample Preparation

Extrusion. A co-rotating Leistritz-double screw extruder ZSE 18HP with a cooled feeder and nine separately heatable blocks is

used. The temperatures for all heating blocks of the extruder were adjusted to 230–240°C. One degassing top each with one oil pump each are joined to blocks 5 and 8. A vacuum of ~ 1 mbar was adjusted. The dosing into the feeder was done volumetrically over a color-exact-dosing instrument. Nanofiller powder was mixed in a Turbula-mixer with milled PBT or PTT. All materials were dried at 130°C for 7 h before extrusion. Storage tanks and dosing instruments were rinsed with 200 L/h nitrogen to minimize thermooxidation. After cooling in water bath cylindrical particles 1.5–2 mm in diameter and 3–4 mm in length were granulated.

Injection Molding. All samples were injection molded after drying (below) with a BOY 22A in combination with the control panel Procan CT. The temperatures of the separable heating zones were 70°C (enter), 230°C (zone 1), 240°C (zone 2), 245°C (zone 3), and 245°C (nozzle) for both PBT and PTT. Clamping forces were 200 kN and 220 kN for PBT and PTT, respectively.

Instrumentation

Elementary Analysis. The composition of the modified clay was analyzed with EA 1110 (CE INSTRUMENTS) used Dynamic Flash Combustion, gas chromatographic column (Porapak PQS) and TCD detector, in combination with Eager 200 or DP 200.

Milling. PBT and PTT were milled before using in a SM 2000-mill of Retsch GmbH, Germany.

Drying. The materials were dried at 130°C over a molecular sieve for 7 h in vacuum.

Water Content. The water contents were analyzed by Karl-Fischer (KF) method, performed with a Karl-Fischer-coulometer 756 in combination with a KF-oven (Metrohm AG).

Pyrolysis. The samples were heated between 300°C and 750°C in 50°C-steps for 30 min, each. Finally, heating was conducted at 750°C for 2 h.

DSC and TGA. Samples were analyzed with TA Instruments DSC Q 1000 and TGA 500. Thermal behavior of the materials was studied in a temperature range of -50°C to 260°C for DSC and -50°C to 550°C for TGA. Heating and cooling was varied with a rate of 10 K/min, each. The following abbreviations are used in the text: melting temperature (T_m), crystallization temperature (T_c), cold crystallization temperature (T_{cc}), enthalpy of fusion (ΔH_m), heat of crystallization (ΔH_c), and heat of cold crystallization (ΔH_{cc}). Furthermore, for the exothermic prepeaks of the melting peaks of the 2. DSC-scans of the PTT-based samples: crystallization temperature (T_{mc}), heat of crystallization (ΔH_{mc}).

The degrees of crystallinity, X_c , are calculated from the absolute values of the exothermic heats ΔH_c according to eq. (1):

$$X_c[\%] = (\Delta H_c / (\Delta H_0(1 - \varphi))) \cdot 100\% \quad (1)$$

where ΔH_0 is the heat of fusion of the completely crystalline polymer. φ means the inorganic part of the nanofiller. The ΔH_0 -values 145.55 J/g and 145.37 J/g of PTT and PBT were calculated from 30 kJ/mol (PTT⁴²) and 32 kJ/mol (PBT⁴³), respectively.

Table I. Composition of the Modified Clay Estimated by Elementary Analysis and TGA

| | Clay |
|-------------------------|-------------------|
| C [%] | 21.87 |
| H [%] | 3.99 |
| N [%] | 0.83 |
| Cl [%] | 0.46 |
| Inorganic component [%] | 75.6 (TGA, 550°C) |
| Organic component [%] | 24.4 (TGA, 550°C) |

Rheology. Melt rheology was studied by means of an Advanced Rheometric Expansion System (ARES, TA Instruments) using parallel plate geometry (25 mm diameter and 1 mm gap). The dried samples (130°C, 7 h, vacuum) were tested at 235°C, under nitrogen atmosphere. Dynamic frequency sweep measurements were performed in the frequency range from 0.1 to 70 s⁻¹ using strain amplitude within the linear viscoelastic regime.

Viscometry. Intrinsic viscosities, $[\eta]$, of the samples were determined by means of the viscosimeter device AVS 250 and the temperature-controlling device CT 1450 of the Schott Geräte GmbH, Germany. The used solvent was a mixture of 1,2-dichlorobenzene and phenol with a weight ratio of 2 : 3; 100 mg of the dried samples, polyester, or composites were weighed and dissolved under gentle heating in the solvent mixture. Measurements were performed at 25°C.

With respect to eq. (2), the relative viscosity, η_{rel} , was determined as a quotient of absolute viscosity (retention time) of the polymer solution $\eta(t)$ and of the pure solvent $\eta_0(t_0)$ in an Ubbelohde viscometer. Specific viscosity, η_{spec} , is defined by $\eta_{rel} - 1$. Single-point eq. (2)⁴⁴ fits the experimental $[\eta]$ -data best.

$$[\eta] = [(1 + 4 \cdot k_H \cdot \eta_{spec})^{0.5} - 1] / (2 \cdot k_H \cdot c) \quad (2)$$

The concentrations c of the polymer solutions were corrected with regard to the experimental amounts of the inorganic filler components. The Huggins constant k_H of the used solvent system is 0.25 ± 0.07 .

Mechanical Testing. Tensile strength and modulus of the materials were measured according to DIN EN ISO 527 and 178, respectively, with a universal testing machine (Zwick 020) using the injection-molded standard test specimen. However, the tensile modulus was determined as the maximum derivative at the beginning of the stress-strain curve measured at 50 mm/min testing speed.

X-ray. WAXD patterns were measured under ambient temperature on a Bruker-AXS D5000 X-ray diffractometer (40 kV, 30 mA) equipped with a CuK α radiation source ($\lambda = 0.15406$ nm) and a Ge(111) crystal monochromator. Samples were scanned in a θ -range between 3 and 8°, with a step size of 0.05° (50 s for every step), using symmetrical transmission technique. The d_{001} based spacings were calculated from the 2θ values.

Scanning Electron Microscopy. Cryo-fractured surfaces were generated by breaking the test bars under liquid nitrogen condi-

tions and subsequent sputtering with Pt with a thickness of 4 nm. Cut surfaces were produced with a Leica RM 2255 (Leica, Germany) vibrating knife perpendicular to the flow direction. The fracture und cut surfaces were studied with an SEM Jeol JSM 6330F (Jeol, Japan) at 5 kV.

Transmission Electron Microscopy. TEM images were taken with a digital camera MegaView II (Olympus, Germany) from cryogenically microtomed ultrathin sections (60 nm), prepared with an UltraCut S (Leica, Germany), with a Phillips CM 200 (Netherlands) at an acceleration voltage of 120 kV.

RESULTS AND DISCUSSION

The Materials

The modified layered silicate belongs to the clay-group of bentonite modified by benzyldimethylstearylammmonium cations. The percentage of the inorganic clay component of the filler depends on the ion exchange capacity and the molecular weight of the modifier (Table I).

By TG analysis it was found that 75.6% of the modified clay are nonvolatile inorganic materials. This result has to be taken into consideration for the preparation of composites with a constant percentage of the inorganic clay component of 3%. Impurities like chloride ions, detected by elementary analysis, were in the order of 0.5%.

Thermal stability of both the modified filler and the corresponding modifier, the organic ammonium chloride, were examined by TG-analysis (Figure 1).

Both benzyl fragmentation and the interactions with the polar clay surface limit the thermal stability of the modified filler. Taking these facts into account, manufacturing of the clay should be focused on a temperature range between 220°C and 230°C.

With regard to sample preparation, it was of prime importance to use a mixture of milled matrix polymers and the filler powder. In contrast to polymer pellets, this way minimized the danger of separation of the material mixture in the storage tank of

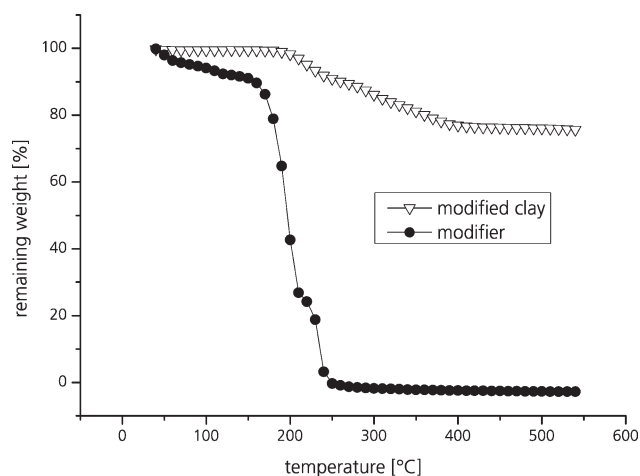
**Figure 1.** Results of TG-analysis of the modified clay and the modifier benzyldimethylstearylammmonium chloride.

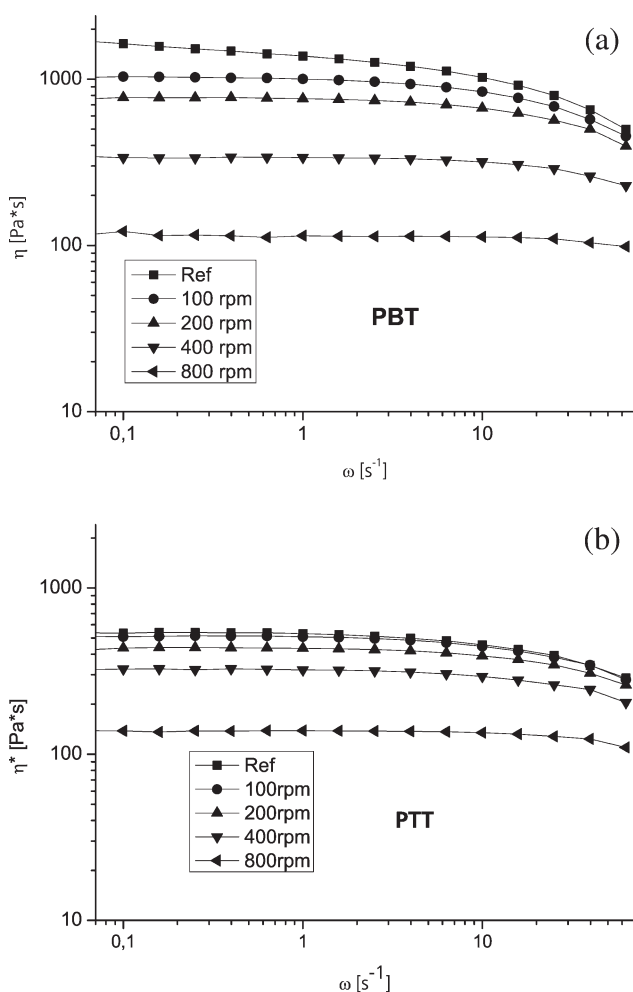
Table II. Water Content of the Polyesters PBT and PTT and the Modified Filler After Drying (130°C, 7 h)

| | PBT | PTT | Clay |
|----------------------|------|------|------|
| H ₂ O [%] | 0.06 | 0.07 | 0.77 |

the extruder. According to Reference 37, the filler content of the composites was limited to 3% of the clay component of the modified clay. To best protect the sensitive aromatic polyesters against hydrolysis the polymers and the filler were dried directly before use. Table II informs about the water contents of the different matrix polymers and the modified filler.

Further reduction of the humidity level of the filler by using higher temperatures for a longer time was not performed due to the beginning of partial degradation of the organic modifier.

In front of composite preparation it is important to study the influence of the extrusion conditions on the properties of the neat polymers. The screw design was characterized by back-mixing elements located in the middle part of the screws and was

**Figure 2.** Change of melt viscosities of neat PBT (a) and neat PTT (b) extruded at different speeds of rotation (100 rpm, 200 rpm, 400 rpm, and 800 rpm).

kept constant for all experiments. This enables an intensive input of mechanical power into the polymer melt. Additionally, vacuum was used to support elimination of oxygen and volatile by-products, mostly represented by monomers and decomposition products of the organic modifier. On the basis of this, the colors of the neat polymers and the composite materials, described in the next chapter, turned to white and pale gray, respectively, and not to yellow–brown. The extrusion temperatures were selected as gentle as possible. Therefore, processing of PBT and PTT was performed at 240°C and 230°C, respectively.

The influence of speeds of rotation of the screws on thermal stability of the neat polyesters was examined at 100 rpm, 200 rpm, 400 rpm, and 800 rpm. Polymer degradation was analyzed by solution viscosity and rheology. Figure 2 presents the influence of processing on the melt viscosities of PBT and PTT.

Degradation of the polymers at speeds of rotation between 100 rpm and 400 rpm was more pronounced for PBT, the polyester with the higher initial melt viscosity. It becomes clear for both polymers that extrusion should be limited to a speed of rotation of 200 rpm to protect them best. Otherwise, manufacturing at 400 rpm was most interesting for an attempt to use a maximum shear stress for intercalation and exfoliation of the filler platelets near the limit of stability of the polymers. Therefore, the materials were extruded at 100 rpm, 200 rpm, and 400 rpm.

The Composites

Preparation. The inorganic filler contents of the composites were determined by pyrolysis experiments (Table III). With regard to the expected filler content of 3% the inorganic clay components scatter within a range between -0.3% and $+0.2\%$. It is noticeable that the samples extruded at 100 rpm contained the highest amounts of clay. It cannot be excluded completely that partial separation between milled polymer and filler powder took place in the storage tank of the extruder during processing. Separation was more drastic by using polymer pellets instead of milled polyesters.

Investigations about the influence of processing and filler on polymer degradation were completed by the analysis of intrinsic viscosities of the neat and manufactured polymers and composites (Table IV).

In accordance with the results of rheology there is a graduation for both neat polymers to lower intrinsic viscosities with rising speeds of rotation of the screws. Although the intrinsic viscosities of PBT and PTT directly correspond to the melt viscosities,

Table III. Content of the Inorganic Components of the Composites Prepared with PBT, PTT, and Modified Clay, Manufactured at Different Speeds of Rotation

| | PBT Clay | PTT Clay |
|---------|-------------|-------------|
| 100 rpm | 3.2% | 3.0% |
| 200 rpm | 2.8% | 2.7% |
| 400 rpm | 2.7% | 2.8% |

Table IV. Intrinsic Viscosities (dL/g) of the Neat Polymers PBT and PTT and the Composites as a Function of Screw Rotation Speed

| Samples | 0 rpm | 100 rpm | 200 rpm | 400 rpm |
|------------|-------|---------|---------|---------|
| PBT (neat) | 1.277 | 1.198 | 1.257 | 0.967 |
| With clay | -- | 0.945 | 0.898 | 0.863 |
| PTT (neat) | 0.977 | 0.976 | 0.969 | 0.921 |
| With clay | -- | 0.879 | 0.895 | 0.834 |

presented by Figure 2, the intrinsic viscosities of the composites show that the filler additionally supports degradation of the aromatic polyesters. The change of intrinsic viscosities is more graduated for the PBT-based composites. PBT shows higher susceptibility to mechanical stress because of the higher melt viscosity in combination with higher degrees of friction and temperature during processing.

Degradation of the polyesters becomes additionally supported if the thermal stability of the modifier is not sufficient. A benzyltrialkylammonium cation was used as modifier for the tested nanofiller. Such organic compounds can be thermally degraded by special fragmentation reactions.⁴⁵ Separation of benzyl groups is preferred due to resonance stabilization effects of the aromatic rings.⁴⁶ Tertiary amines should be mainly formed, in accordance with Hofmann degradation reactions.⁴⁷ Such strongly basic aliphatic amines are very reactive and are preferred for polymer degradation.⁴⁸

Thermoanalytical Investigations

The influence of processing and the filler on melt and crystallization parameters (T_c , T_m , ΔH_m , ΔH_c , X_c) was examined by DSC investigations. Data for PBT and PTT are separately presented in Tables V and VI, respectively. Furthermore, the data of the first and second DSC run (heating and cooling) are shown in each case.

For PBT, the different processing conditions do not influence the melting temperatures significantly. T_m values range between 223°C and 225°C nearly unchanged. The crystallization temperatures (T_c) of the composites rise marginally between 190°C

and 193°C. Such shifts indicate nucleating effects of the nanofiller. The small magnitude of this effect can be attributed to the high crystallization rate of neat PBT, in contrast to other aromatic polyesters like PTT and PET.⁴⁹ There are no significant differences between T_m and T_c of the first and second DSC-run.

Although enthalpies of melting and crystallization, associated with the first DSC scan, are nearly identical (Table V), heat of fusion of the second DSC-run shows differences. The values are smaller than the corresponding data of the first DSC-scans (34–40 J/g) but are necessarily in a typical range of conventionally produced PBT (35–50 J/g).⁵⁰ Second heating is characterized by the detection of multiple melting peaks (Figure 3).

In the case of PBT, multiple endotherms can be attributed to complex multistep processes of recrystallization and remelting.^{51,52} With respect to PTT, melting temperatures of PTT and PTT-based nanocomposites remain unchanged (226–228°C) and do not depend on sample history (Table VI).

In contrast, crystallization temperatures of processed neat PTT-samples and composites increase with respect to the unprocessed sample by 13–25°C. This is more than ΔT_c values of 14–15°C published by Cho et al.⁵³ T_c data of the second exotherms are more graduated, they correlate weakly inverse with the intrinsic viscosities of the PTT-samples (Figure 4).

Such a trend is confirmed by Chen et al.⁵⁴ and reveals that the crystallization rate of PTT increases with decreasing molecular weights of PTT. Furthermore, the addition of the nanofiller is associated with nucleating actions of the modified clay so that the higher-than-average shifts of T_c -values seem to be a superposition of these two factors.

In comparison with PBT, there are differences in the thermograms of the PTT-samples (Figure 5). Cold crystallization between 57°C and 65°C is shown for the first DSC-run (T_{cc} , ΔH_{cc}). The endotherm of the second DSC-scan is characterized by a small exothermic prepeak (T_{mc} , ΔH_{mc}) between 201°C and 215°C (Table VI). Cold crystallization of the PTT-samples can be attributed to the lower crystallization rate of PTT in contrast to PBT.⁴⁹ The absolute enthalpy values of cold crystallization

Table V. Selected Results of DSC-Investigations of the PBT-Based Samples, First and Second Run, $r = 10$ K/min

| | PBT | PBT/100 | PBT/200 | PBT/400 | PBT/clay/100 | PBT/clay/200 | PBT/clay/400 |
|----------------------|-----|---------|---------|---------|--------------|--------------|--------------|
| 1. Cyclus | | | | | | | |
| T_m [°C] | 225 | 224 | 224 | 225 | 224 | 224 | 225 |
| ΔH_m [J/g] | 51 | 49 | 47 | 55 | 46 | 46 | 52 |
| T_c [°C] | 190 | 188 | 189 | 190 | 191 | 192 | 193 |
| $ \Delta H_c $ [J/g] | 46 | 48 | 46 | 51 | 45 | 46 | 50 |
| X_c [%] | 32 | 33 | 32 | 35 | 31 | 32 | 34 |
| 2. Cyclus | | | | | | | |
| T_m [°C] | 224 | 223 | 223 | 224 | 224 | 223 | 224 |
| ΔH_m [J/g] | 38 | 37 | 35 | 40 | 34 | 35 | 39 |
| T_c [°C] | 189 | 188 | 188 | 190 | 191 | 192 | 193 |
| $ \Delta H_c $ [J/g] | 43 | 47 | 46 | 51 | 46 | 48 | 50 |
| X_c [%] | 30 | 32 | 32 | 35 | 32 | 33 | 34 |

Table VI. Selected Results of DSC-Investigations of the PTT-Based Samples, First and Second Run, $r = 10$ K/min

| | PTT | PTT/100 | PTT/200 | PTT/400 | PTT/clay/100 | PTT/clay/200 | PTT/clay/400 |
|-----------------------------|-----|---------|---------|---------|--------------|--------------|--------------|
| 1. Cyclus | | | | | | | |
| T_{cc} [°C] | 57 | 66 | 65 | 65 | 62 | 64 | 64 |
| $Y = \Delta H_{cc} $ [J/g] | 4 | 8 | 11 | 11 | 12 | 12 | 11 |
| T_m [°C] | 227 | 227 | 227 | 228 | 227 | 227 | 227 |
| ΔH_m [J/g] | 60 | 56 | 61 | 63 | 58 | 57 | 56 |
| $\Delta H_m - Y$ [J/g] | 56 | 48 | 50 | 52 | 46 | 45 | 45 |
| T_c [°C] | 164 | 182 | 182 | 177 | 189 | 188 | 188 |
| $ \Delta H_c $ [J/g] | 45 | 45 | 49 | 50 | 50 | 49 | 49 |
| X_c [%] | 31 | 31 | 34 | 34 | 34 | 34 | 34 |
| 2. Cyclus | | | | | | | |
| T_{mc} [°C] | 201 | 211 | 211 | 206 | 215 | 214 | 214 |
| $ \Delta H_{mc} $ [J/g] | 5 | 4 | 4 | 6 | 1 | 1 | 1 |
| T_m [°C] | 227 | 226 | 226 | 227 | 226 | 227 | 227 |
| ΔH_m [J/g] | 52 | 44 | 48 | 53 | 42 | 45 | 44 |
| T_c [°C] | 164 | 179 | 179 | 177 | 188 | 187 | 187 |
| $ \Delta H_c $ [J/g] | 42 | 43 | 48 | 48 | 48 | 48 | 47 |
| X_c [%] | 29 | 30 | 33 | 33 | 33 | 33 | 32 |

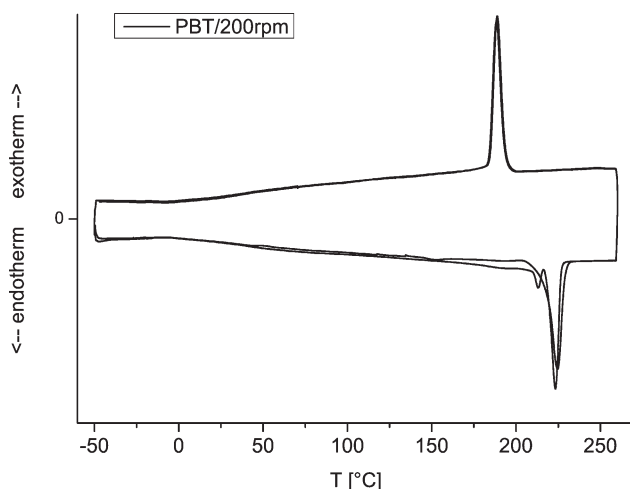
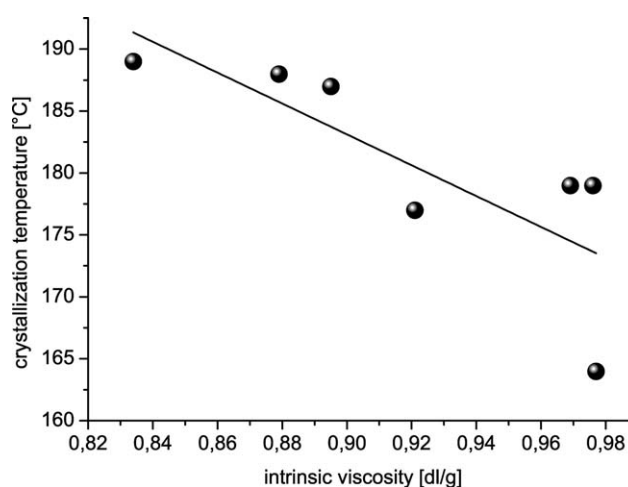
and melt crystallization of the first DSC-run have mostly the same magnitude as the corresponding heats of fusion of the first scan.

Heat of fusion of the first and second DSC-run are essentially characterized by a drop of ΔH_m between unprocessed neat PTT and PTT/100. This effect can be finally attributed to the intact polymer chains of PTT in front of processing, in accordance with the results published by Chen et al.,⁵⁴ and the unknown thermal history of the virgin polyester. Compared with PTT/100, the slightly increasing ΔH_m values of PTT/200 and PTT/400 indicate the ability of processed neat PTT, partially degraded polymers (Table IV), to form slightly increased

degrees of crystallinity (Table VI). Such an effect results finally from correlations as presented in Figure 4.

For both PBT- and PTT-based materials, there are no significant differences between X_c -data of the first and second DSC-scan. X_c -values of the composites are only slightly higher than the X_c -data of neat polymers processed at 100 rpm. Compared with the reference materials, unprocessed neat polyesters, this means an increase of X_c from 30% to 35% (Table V, 2. Cyclus) and from 29% to 33% (Table VI, 2. Cyclus) for PBT and PTT, respectively.

With respect to glass-transition temperatures, extrusion of neat PTT decreases the T_g value slightly from 51°C to a temperature range between 48°C and 49°C (Table VII).

**Figure 3.** First and second DSC-run of neat PBT processed at 240°C and 200 rpm.**Figure 4.** Correlation between intrinsic viscosities of the PTT-based samples and their crystallization temperatures (2. DSC-run), $r = 10$ K/min.

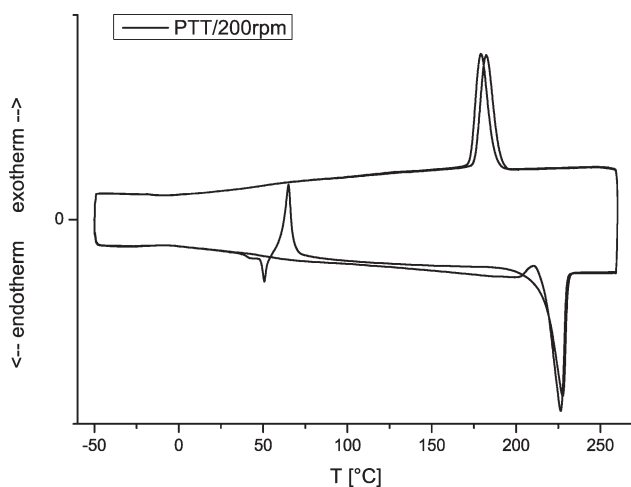


Figure 5. First and second DSC-run of neat PTT processed at 230°C and 200 rpm.

Glass-transition temperatures of the corresponding PTT-composites are slightly higher (49–51°C) and indicate a marginally positive effect of the filler. T_g of unprocessed neat PBT could not be detected. There is no influence of the different processing conditions (rpm) on glass-transition temperatures of processed neat PBT. Only the composite PBT/Nanofil2/400 rpm shows a marginally higher T_g value.

Rheology

The interactions between matrix polymers and nanofiller in the polymer melt were examined by rheology. Figure 6 presents the bi-logarithmic plots of complex viscosity versus ω of neat PBT and PTT and the corresponding composites loaded with 3% modified clay.

Figure 6 reveals a significant difference between the virgin polyesters and the nanocomposites. In contrast to the neat polymers PBT and PTT, the composites show strong non-Newtonian behavior, with a small benefit for the PTT-based samples. Storage modulus, G' , is more sensitive towards dispersed morphology in the molten state and exposes this difference more clearly. Figure 7 highlights the influence of clay on the melts of PBT and PTT by a G' - ω -plot.

The difference in the low- ω -zone behavior may be due to different extents of exfoliation of the clay particles and the different melt viscosities of the matrix polymers. The low-viscosity PTT-melt becomes clearly more changed by the nanofillers. In contrast, the higher viscose PBT melt compensates the filler effects.

Table VII. Glass-Transition Temperatures (T_g) of Neat and Processed Polymers and Composites; 2. Scan, $r = 10$ K/min

| | 0 rpm | 100 rpm | 200 rpm | 400 rpm |
|--------------|-------|---------|---------|---------|
| PTT | 51 | 48 | 49 | 48 |
| PTT/Nanofil2 | | 51 | 49 | 49 |
| PBT | -- | 41 | 41 | 41 |
| PBT/Nanofil2 | | 40 | 39 | 42 |

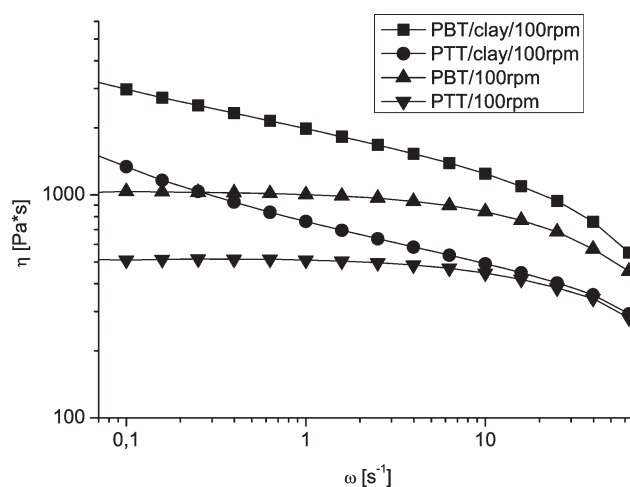


Figure 6. Melt viscosities of neat PBT and PTT and the composites loaded with modified clay (3%), $T = 235^\circ\text{C}$.

X-ray

To obtain more detailed information about the extent of exfoliation, the influence of PBT and PTT on the modified clay during processing was investigated by X-ray analysis (Figure 8).

The unprocessed nanofiller was examined as a macroscopic mixture between filler and PTT prepared for composite formation. Therefore, all samples (mixture and composites) contained comparable amounts of the inorganic component of the modified clay (Table III). The modifier of the clay, benzyldimethylstearylammmonium cations, influences both the interlayer distance of the modified filler (1.8 nm) and the physical interactions to the polymer matrix by the length of the alkyl chains and their hydrophobic properties, respectively.

The polyesters support exfoliation of the clay platelets differently. In contrast to the PTT-composite, the clay-peak disappeared by the application of PBT. The higher melt viscosity of PBT in contrast to PTT can be assumed as an important reason for that. The peak of the detectable filler material of the PTT-composite is shifted to higher 2θ -values, indicating a decrease

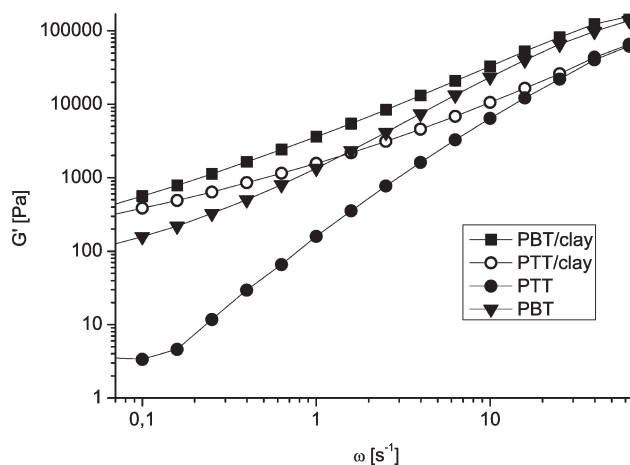


Figure 7. Influence of the clay on the storage modulus of PBT and PTT, $T = 235^\circ\text{C}$.

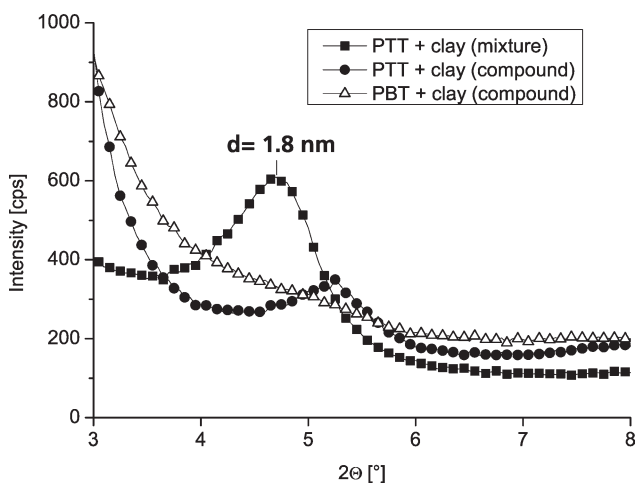


Figure 8. WAXD patterns of composites made from PBT, PTT and modified clay (3%), processed at 200 rpm, and of a mixture of PTT and clay (3%) before processing.

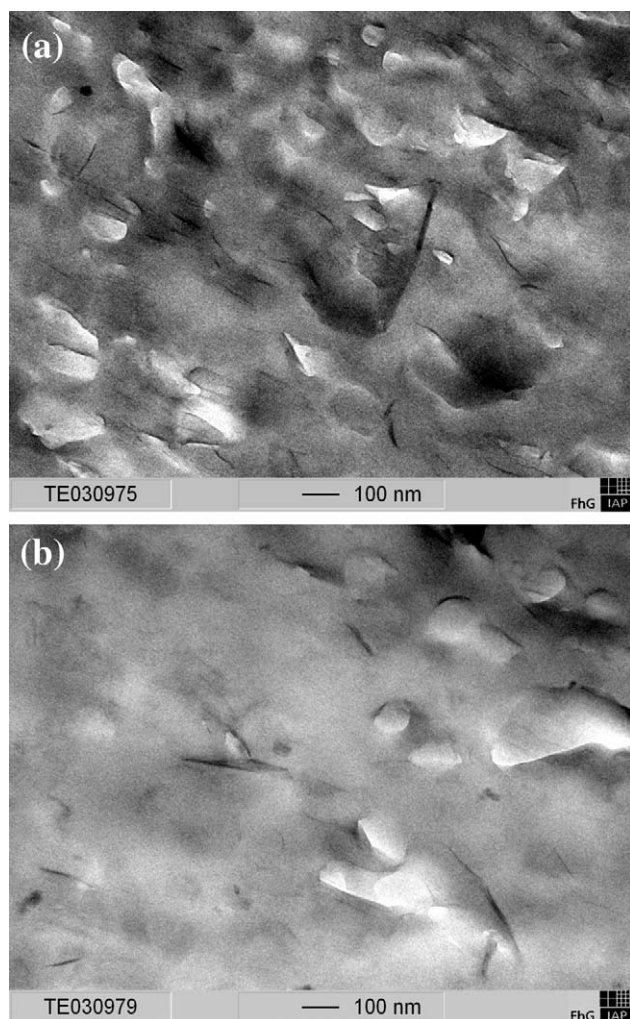


Figure 9. TEM-micrographs of a PBT-composite (a) and a PTT-composite (b) loaded with modified clay (3%, effective) and extruded at 200 rpm.

Table VIII. Results of Tensile Tests, Dry Samples Stored at Room Temperature

| Samples | σ_{\max} [MPa] | ε_{\max} [%] | E [MPa] |
|-------------------|-----------------------|--------------------------|-----------|
| PBT 6550 | 52.2 ± 0.9 | 3.4 ± 0.1 | 2130 ± 10 |
| PBT 100rpm | 54.0 ± 0.6 | 3.7 ± 0.1 | 1920 ± 40 |
| PBT 200rpm | 54.4 ± 0.7 | 3.7 ± 0.1 | 1980 ± 80 |
| PBT 400rpm | 56.7 ± 0.2 | 8.5 ± 0.3 | 2070 ± 60 |
| PBT+3%clay/100rpm | 61.1 ± 0.3 | 4.5 ± 0.6 | 2660 ± 30 |
| PBT+3%clay/200rpm | 61.2 ± 0.7 | 4.4 ± 0.3 | 2650 ± 20 |
| PBT+3%clay/400rpm | 60.6 ± 0.9 | 3.1 ± 0.1 | 2660 ± 20 |
| PTT | 60.5 ± 0.5 | 6.4 ± 0.6 | 2080 ± 50 |
| PTT 100rpm | 65.9 ± 0.6 | 4.8 ± 0.9 | 2350 ± 20 |
| PTT 200rpm | 65 ± 1.0 | 4.1 ± 0.1 | 2350 ± 40 |
| PTT 400rpm | 64.3 ± 0.6 | 4.0 ± 0.1 | 2330 ± 10 |
| PTT+3%clay/100rpm | 54.2 ± 2.0 | 2.2 ± 0.3 | 2790 ± 40 |
| PTT+3%clay/200rpm | 57.6 ± 2.5 | 2.3 ± 0.2 | 2810 ± 20 |
| PTT+3%clay/400rpm | 54.2 ± 1.7 | 2.2 ± 0.1 | 2760 ± 30 |

of the interlayer distance from 1.8 nm to 1.68 nm for a part of the modified filler; the main part seems to be exfoliated (Figures 8 and 9). Such an effect can be attributed to compression of the clay layers under mechanical stress during processing if the melt viscosity of the matrix polymer is not sufficient for exfoliation. The modifier is pressed out of the galleries and can't support platelet separation.

Morphology

The dispersed fillers in the composites made from PBT, PTT, and modified clay were detected by TEM imaging [Figure 9(a,b), respectively]. The micrographs illustrate a typical intercalated structure. The average thickness and length of the dispersed silicates are about 10–20 nm and 100–250 nm, respectively.

Mechanical Investigations

The efficiency of the filler to enhance the mechanical properties of the composites was studied by tensile tests of samples handled under dry conditions at room temperature; Table VIII presents selected results.

Partial degradation of the matrix polymers during processing affects their mechanical properties. In the case of extruded neat PBT-samples there was a weak increase of tensile strength with rising speed of rotation from 52.2 MPa for non manufactured PBT to 56.7 MPa. The modulus was slightly reduced from 2130 MPa to 1920 MPa–2070 MPa. Change of elongation remained almost uninfluenced at ~ 3.5%. Extrusion of virgin PTT enhanced tensile strength from 60.5 MPa to ~ 65 MPa. Young's modulus changed from 2080 MPa to 2350 MPa. This means an increase in stiffness which is also indicated by a decrease of ε from 6.4% to 4%. The improved tensile strength of the processed neat polymers seems to correlate with the slightly enhanced degree of crystallinity (Tables V and VI). This effect can also be explained by an increase of X_c with decreasing polymer molecular weight.⁵⁴

The presence of the modified clay during extrusion changed these results as follows. For PTT, Young's modulus could be improved in the range between 17% and 19%, with regard to

the values of manufactured neat PTT (2350 MPa). There is a loss of tensile strength in an order of magnitude of 11–17%, compared with the corresponding data of the manufactured neat samples.

A small fraction of not completely exfoliated nanofiller particles, identified by X-ray analysis (Figure 8), can act as defects in these PTT-nanocomposites. They increase material stiffness but decrease resistance against tensile impacts. Obviously, the low-viscose PTT-melts (Table IV) does not exfoliate the modified clays as effective as in the case of the high-viscose PBT-melts. Therefore, application of high-molecular PTT seems to be an interesting alternative. To get high-molecular PTT, the commercially available PTT can be subjected to solid-state polycondensation.⁵⁵

In contrast, all PBT composites are characterized by Young's moduli of ~ 2650 MPa. This means an increase of 28–38%, with regard to the neat samples. Additionally, tensile strength could be substantially enhanced. This means an improvement of nearly 13% especially for the composites extruded at 100 rpm and 200 rpm. These facts clarify the graduation between the different influences of both thermoplastic processing and the presence of the filler on the properties of the composite materials.

CONCLUSIONS

Two types of nanocomposites have been prepared with PBT (extrusion type) and PTT as polymer matrix materials, loaded with 3% modified clay via melt compounding in a twin-screw extruder. The clay was modified with benzyldimethylstearyl ammonium cations.

The extrusion chamber has to be rinsed with nitrogen under reduced pressure to protect the polyester melts against oxidative degradation by oxygen and to remove volatile by products. Extrusion of PBT and PTT was performed best at 240°C and 230°C, respectively. The most effective speeds of rotation of the screws ranged between 100 rpm and 200 rpm. Melt viscosities of nearly 800 Pa*s and 430 Pa*s for neat PBT and PTT (200 rpm), respectively, were detected.

Both processing and the presence of the nanofiller degrade the polymers, but in a different order of magnitude. Intrinsic viscosity (IV) of neat PBT manufactured at 200 rpm has been decreased from 1.277 dL/g (not manufactured) to 1.257 dL/g. The nanofiller stimulated further decomposition indicated by a drop of IV to 0.898 dL/g (200 rpm). The corresponding results for PTT are 0.977 dL/g (neat PTT), 0.969 dL/g (neat PTT, 200 rpm), and 0.895 dL/g (PTT composite, 200 rpm).

X-ray analysis reveals a small fraction of nonexfoliated clay in the PTT-composites with consequences for their mechanical properties. Although material stiffness increased from 2.35 GPa to 2.81 GPa (200 rpm), tensile strength was reduced from 65.0 MPa to 57.6 MPa (200 rpm). Particles not completely exfoliated acted as defects. In contrast to these results, an increase of tensile strength from 54.4 MPa to 61.2 MPa was observed for the material combination PBT/ modified clay (200 rpm); Young's modulus was enhanced from 1.98 GPa to 2.65 GPa.

The better results for PBT can be attributed to the higher melt viscosity of this polyester, sufficient to support melt intercala-

tion and exfoliation in contrast to the PTT case. In preparation of further experiments, PTT will be subjected to solid-state-polycondensation (SSP) before nanocomposite preparation to enhance melt viscosity by increased average molecular weight.

REFERENCES

1. Cheng-Fang, O. *J. Polym. Sci. Part B: Polym. Phys.* **2003**, *41*, 2902.
2. Cheng-Fang, O. *J. Appl. Polym. Sci.* **2003**, *89*, 3315.
3. Chang, J.-H.; Mun, M. K.; Kim, J.-Ch. *J. Appl. Polym. Sci.* **2006**, *102*, 4535.
4. Kim, K. J.; Ramasundaram, S.; Lee, J. S. *Polym. Compos.* **2008**, *29*, 894.
5. Cho, H. W.; Lee, J. S.; Prabu, A. A.; Kim, K. J. *Polym. Compos.* **2008**, *29*, 1328.
6. Russo, G. M.; Simon, G. P.; Incarnato, L. *Macromolecules* **2006**, *39*, 3855.
7. Kim, J. Y.; Han, S. I.; Hong, S. *Polymer* **2008**, *49*, 3335.
8. Kim, N. H.; Malhotra, S. V.; Xanthos, M. *Microporous Mesoporous Mater.* **2006**, *96*, 29.
9. Vaia, R. A.; Teukolsky, R. K.; Giannelis, E. P. *Chem. Mater.* **1994**, *6*, 1017.
10. Gurmendi, U.; Eguiazabal, J. I.; Nazabal, J. *Eur. Polym. J.* **2008**, *44*, 1686.
11. Zhu, J.; Morgan, A. B.; Lamelas, F. J.; Wilkie, C. A. *Chem. Mater.* **2001**, *13*, 3774.
12. Gilman, J. W.; Awad, W. H.; Davis, R. D.; Shields, J.; Harris, R. H., Jr.; Davis, C.; Morgan, A. B.; Sutto, T. E.; Callahan, J.; Trulove, P. C.; DeLong, H. C. *Chem. Mater.* **2002**, *14*, 3776.
13. Fornes, T. D.; Yoon, P. J.; Hunter, D. L.; Keskkula, H.; Paul, D. R. *Polymer* **2002**, *43*, 5915.
14. Stoeffler, K.; Lafleur, P. G.; Denault, J. *Polym. Degrad. Stab.* **2008**, *93*, 1332.
15. Ray, S. S.; Okamoto, M. *Prog. Polym. Sci.* **2003**, *28*, 1539.
16. Ray, S. S.; Bousmina, M. *Prog. Mater. Sci.* **2005**, *50*, 962.
17. Maiti, P.; Batt, C. A.; Giannelis, E. P. *Polym. Mater. Sci. Eng.* **2003**, *88*, 58.
18. Park, H. M.; Li, X.; Chang-Zhu, J.; Park, C. Y.; Cho, W. J.; Ha, C. K. *Macromol. Mater. Eng.* **2002**, *287*, 553.
19. Ray, S. S.; Okamoto, K.; Yamada, K.; Okamoto, M. *Nano Lett.* **2002**, *2*, 423.
20. Kato, M.; Usuki, A.; Okada, A. *J. Appl. Polym. Sci.* **1997**, *66*, 1781.
21. Rong, J.; Jing, J.; Li, H.; Sheng, M. A. *Macromol. Rapid Commun.* **2001**, *22*, 329.
22. Wang, Z.; Pinnavaia, T. J. *Chem. Mater.* **1998**, *10*, 3769.
23. Huang, X.; Lewis, S.; Brittain, W. J.; Vaia, R. A. *Macromolecules* **2000**, *33*, 2000.
24. Bourbigot, S.; Vanderhart, D. L.; Gilman, J. W.; Awad, W. H.; Davis, R. D.; Morgan, A. B.; Wilkie, C. A. *J. Polym. Sci. Part B: Polym. Phys.* **2003**, *41*, 3188.

25. Kojima, Y.; Usuki, A.; Kawasumi, M.; Fukushima, Y.; Okada, A.; Kurauchi, T.; Kamigaito, O. *J. Mater. Res.* **1993**, *8*, 1179.
26. Hasegawa, N.; Okamoto, H.; Kato, M.; Usuki, A.; Sato, N. *Polymer* **2003**, *44*, 2933.
27. Chang, J.-H.; Kim, S. J.; Im, S. *Polymer* **2004**, *45*, 5171.
28. Wu, D.; Zhou, Ch.; Zhang, M. *J. Appl. Polym. Sci.* **2006**, *102*, 3628.
29. Zhanga, G.; Shichia, T.; Takagi, K. *Mater. Lett.* **2003**, *57*, 1858.
30. Glenz, W. *Kunststoffe* **2007**, *10*, 76.
31. Wijayathunga, V. N.; Lawrence, C. A.; Blackburn, R. S.; Bandara, M. P. U.; Lewis, E. L. V.; El-Dessouky, H. M.; Cheung, V. *Opt. Laser Technol.* **2007**, *39*, 1301.
32. Eipper, A. *Kunststoffe* **2007**, *10*, 120.
33. Chuah, H. H. Paper presented at Tifcon '96, The Textile Institute, Blackpool, UK, Nov. 6, **1996**.
34. Kurian, J. V. *J. Polym. Environ.* **2005**, *13*, 159.
35. Kim, T.-K.; Son, Y.-A.; Lim, Y.-J. *Dyes Pigm.* **2005**, *67*, 229.
36. Run, M.; Yao, Ch.; Wang, Y.; Gao, J. *J. Appl. Polym. Sci.* **2007**, *106*, 1557.
37. Hu, X.; Lesser, A. J. *J. Polym. Sci. Part B: Polym. Phys.* **2003**, *41*, 2275.
38. Liu, Z.; Kequan Chen, K.; Yan, D. *Eur. Polym. J.* **2003**, *39*, 2359.
39. Liu, Z.; Chen, K.; Yan, D. *Polym. Test.* **2004**, *23*, 323.
40. Drown, E. K.; Mohanty, A. K.; Parulekar, Y.; Hasija, D.; Harte, B. R.; Misra, M.; Kurian, J. V. *Compos. Sci. Technol.* **2007**, *67*, 3168.
41. Carroccio, S.; Rizzarelli, P.; Scaltro, G.; Puglisi, C. *Polymer* **2008**, *49*, 3371.
42. Pyda, M.; Boller, A.; Grebowicz, J.; Chuah, H.; Lebedev, B. V.; Wunderlich, B. *J. Polym. Sci. Part B: Polym. Phys.* **1998**, *36*, 2499.
43. Cheng, S. Z. D.; Pan, R.; Wunderlich, B. *Macromol. Chem.* **1988**, *189*, 2443.
44. Liu, Y. *Macromol. Mater. Eng.* **2001**, *286*, 611.
45. Xie, W.; Gao, Z.; Liu, K.; Pan, W.-P.; Vaia, R.; Hunter, D.; Singh, A. *Thermochim. Acta* **2001**, *367-368*, 339.
46. Cervantes-Uc, J. M.; Cauich-Rodriguez, J. V.; V'azquez-Torres, H.; Garfias-Mesias, L. F.; Donald, R.; Paul, D. R. *Thermochim. Acta* **2007**, *457*, 92.
47. Haskins, N. J.; Mitchell, R. *Analyst* **1991**, *116*, 901.
48. Buxbaum, L. H. *Angew. Chem. Int. Ed.* **1968**, *7*, 182.
49. Chuah, H. H. *Polym. Eng. Sci.* **2001**, *41*, 308.
50. Brunelle, D. J. In *Modern Polyesters: Chemistry and Technology of Polyesters and Copolyesters*; Scheirs, J., Long, T. E., Eds.; Wiley: New York, **2003**.
51. Righetti, M. C.; Di Lorenzo, M. L. *J. Polym. Sci. Part B: Polym. Phys.* **2004**, *42*, 2191.
52. Mohd Ishak, Z. A.; Gatos, K. G.; Karger-Kocsis, J. *J. Polym. Eng. Sci.* **2006**, *46*, 743.
53. Cho, H. W.; Lee, J. S.; Prabu, A. A.; Kim, K. *J. Polym. Compos.* **2008**, *29*, 1329.
54. Chen, X.; Hou, G.; Chen, Y.; Yang, K.; Dong, Y.; Zhou, H. *Polym. Test.* **2007**, *26*, 144.
55. Kim, S. H.; Kim, J. H. *Fibers Polymers* **2010**, *11*, 170.